ELSEVIER

NeuroImage

www.elsevier.com/locate/ynimg
NeuroImage 40 (2008) 59–67

Improved cortical-layer specificity of vascular space occupancy fMRI with slab inversion relative to spin-echo BOLD at 9.4 T

Tao Jin[a,*] and Seong-Gi Kim[a,b]

[a]*Department of Radiology, University of Pittsburgh, 3025 East Carson Street, University of Pittsburgh, Pittsburgh, PA 15203, USA*
[b]*Department of Neurobiology, University of Pittsburgh, Pittsburgh, PA, USA*

Received 21 September 2007; revised 7 November 2007; accepted 30 November 2007
Available online 8 December 2007

Cerebral blood volume (CBV)-weighted endogenous functional contrast can be obtained by the vascular space occupancy (VASO) technique. VASO relies on nonselective inversion for nulling blood signals, but the implementation of VASO at magnetic fields higher than 3 T is difficult due to converging T_1 values of tissue and blood water and a stronger counteracting blood oxygen level-dependent (BOLD) effect. To improve functional CBV sensitivity, we proposed to use VASO with *s*lab-selective *i*nversion (SI-VASO). Computer simulations showed that the SI-VASO approach significantly increases functional sensitivity compared to the original VASO in a stronger magnetic field with a shorter repetition time. To examine layer-dependent specificity, SI-VASO and spin-echo BOLD (SE-BOLD) functional magnetic resonance imaging (fMRI) experiments were performed on isoflurane-anesthetized cats during visual stimulation at 9.4 T. Unlike simultaneously acquired SE-BOLD signal, the SI-VASO signal peaked at 0.9 mm from the surface of the cortex and was localized to the middle cortical layer. The full-width at half maximal response across the cortex was narrower for SI-VASO than for SE-BOLD (1.7 mm vs. 2.5 mm, respectively), suggesting that SI-VASO is better localized to neuronally active sites than SE-BOLD fMRI. The magnitude of the SI-VASO change in the middle cortex was −1.45% with our experimental parameters, corresponding to a relative CBV change of ~8% when baseline CBV was assumed to be 5% in a two-compartment model. The signal response profile across the cortex, the calculated CBV change, and the time course of SI-VASO fMRI were similar to those of previously obtained CBV-weighted fMRI with contrast agent in the same animal model, suggesting that SI-VASO measures predominately functional CBV responses.

Keywords: functional MRI; neuronal activity; cortical lamina; cerebral blood volume; CBV; VASO; high magnetic field; spin-echo BOLD

Introduction

Cerebral blood volume (CBV)-weighted functional magnetic resonance imaging (fMRI) using long blood half-life contrast agents has often been applied in animals due to both high sensitivity and its ability to suppress signals from large vessels (Kennan et al., 1998; Kim and Ugurbil, 2003; Mandeville et al., 1998, 1999; Vanduffel et al., 2001), making CBV an appealing fMRI methodology for animal research. Furthermore, CBV-weighted fMRI shows high specificity for neuronally active sites. The highest CBV response is localized at middle cortical layer, where microvessel density, metabolic response, and synaptic inputs are greatest (Harel et al., 2006; Lu et al., 2004b; Zhao et al., 2006), and at "active" orientation-selective columns where activation-induced neural activity is greatest (Fukuda et al., 2006; Zhao et al., 2005). These findings indicate that CBV-based fMRI may be an attractive approach for high-resolution fMRI studies in humans. However, despite that a bolus injection of Gd-DTPA was used in the first fMRI study in human visual cortex (Belliveau et al., 1991), the application of long half-life blood-pool contrast agents to human fMRI research is currently not available due to its invasiveness.

The vascular space occupancy-dependent (VASO) technique was recently proposed for obtaining endogenous CBV-weighted contrast (Donahue et al., 2006; Lu et al., 2003, 2004a). VASO images are acquired by an inversion recovery (IR) sequence, usually at the zero-crossing point of blood water magnetization (i.e. the blood nulling point). When a relatively short repetition time (e.g. TR <3 s) is used for fMRI applications, the sensitivity of VASO is reduced because tissue water magnetization is closer to zero at the blood nulling points with shorter TRs. This problem is exacerbated with higher magnetic fields, where T_1 values of blood and tissue water are longer and relatively closer. For example, with blood and tissue water T_1 values of 2.2 and 1.9 s at 9.4 T (Tsekos et al., 1998), the nulling points of tissue and blood water are 0.865 and 0.912 s for a TR value of 2.5 s, respectively. When the blood is nulled with an inversion time (TI) of 0.912 s, the tissue signal is only 0.026 M_0. An additional difficulty with higher magnetic fields is the increased BOLD signal, which counteracts the negative VASO signal changes and further reduces its sensitivity. To improve VASO sensitivity in high magnetic fields (>3 T), we recently proposed using slab-selective inversion rather than nonselective inversion (Jin and Kim, 2006). If the inversion slab thickness could be optimized, such that fresh blood water from outside the inversion slab arrives at the

* Corresponding author. Fax: +1 412 383 6799.
E-mail address: taj6@pitt.edu (T. Jin).
Available online on ScienceDirect (www.sciencedirect.com).

1053-8119/$ - see front matter © 2007 Elsevier Inc. All rights reserved.
doi:10.1016/j.neuroimage.2007.11.045

imaging slice after each image acquisition and then fills the vasculature before the application of the next inversion pulse, inflowing fresh blood will replace steady-state blood magnetization in the imaging slice during each repetition of IR. This approach is referred to as the slab-inversion VASO (SI-VASO) technique, differentiating it from the original VASO approach. The blood nulling point in SI-VASO images is 0.69 T_1 (1.52 s at 9.4 T) regardless of TR values. Consequently, the signal-to-noise ratio (SNR) for SI-VASO increases because the baseline tissue longitudinal magnetization for TR = 2.5 s becomes 0.31 M_0 at blood-nulling, an order of magnitude greater than that with the original VASO (0.026 M_0). In our preliminary 9.4 T stimulation study (Jin and Kim, 2006), decreases in functional SI-VASO signal were observed with TR = 3 s and TI = 1.5 s, despite significant BOLD contaminations from a relatively long echo time (TE) of 19 ms.

VASO contrast is supposed to be weighted by CBV changes, and thus should have spatial specificity and temporal characteristics similar to contrast agent-based CBV-fMRI studies. Currently, the spatial specificity of VASO-fMRI in previous human studies is not known because of limited spatial resolution. The onset time (or the rising time) of the VASO signal (Lu et al., 2004a; Yang et al., 2004) in humans were found to be faster than those of the BOLD responses, in contrast to CBV responses obtained with monocrystalline iron oxide nanoparticle (MION) in rats and nonhuman primates which were slower than BOLD (Leite et al., 2002; Mandeville et al., 1998). It is currently unclear whether this apparent discrepancy is related to differences in species (human vs. animal) and stimulation, or due to different signal sources of the two techniques (complex source including CBV (Donahue et al., 2006) vs. total CBV). Therefore, it is important to compare the temporal dynamics of the VASO signal with contrast agent-based CBV-fMRI in the same experimental model. In this work, SI-VASO experiments were performed at 9.4 T with a short TE to reduce BOLD contamination. Spatial and temporal characteristics of SI-VASO signals were compared to those of simultaneously acquired spin-echo (SE)-BOLD fMRI, and also with contrast agent-based CBV-weighted fMRI results previously obtained from our group (Zhao et al., 2006).

Materials and methods

Theoretical background of SI-VASO

A nonselective (whole body) inversion is assumed in the original VASO technique. Therefore, inflow contribution to T_1-weighted VASO images is minimal. Ignoring blood–tissue water exchange, the longitudinal magnetizations of tissue and blood water spins at a given TI and TR will reach their respective steady state condition. In a two-compartment model, the signal intensity in an imaging voxel can be expressed as:

$$S = \sum_{i=\text{tissue,blood}} v_i \cdot \rho_i \cdot M_{z,i} \cdot \exp(-TE/T^*_{2,i}), \quad (1)$$

where v is the volume fraction of the corresponding compartment in the voxel, ρ is the proton density, M_z is the longitudinal magnetization, TE is the echo time, and T_2^* is the apparent transverse relaxation time for gradient echo measurements. At a steady state condition, M_z of tissue water will be $(1-2\,e^{-\mathrm{TI}/\mathrm{T}_{1,t}}+e^{-\mathrm{TR}/\mathrm{T}_{1,t}})$, where $T_{1,t}$ is the T_1 value of tissue water.

When the inversion slab thickness is limited, such as in the use of a head coil (rather than a whole body coil), fresh blood water spins outside of the inversion slab can flow into the imaging slice depending on slab thickness and blood velocity. At least three scenarios should be considered: (i) If the fresh spins with magnetization M_0 do not travel into the imaging slice during the whole TR period in case of a thick slab and/or short TR, M_z of blood will be $(1-2\,e^{-\mathrm{TI}/\mathrm{T}_{1,b}}+e^{-\mathrm{TR}/\mathrm{T}_{1,b}})$ where $T_{1,b}$ is the T_1 value of blood water. This condition is the basis of the original VASO technique. (ii) If fresh spins travel into the imaging slice before TI in case of a thin slab and/or long TI, M_z of blood will be the fully relaxed magnetization, M_0. The image contrast is heavily weighted by blood flow, which is the basis of arterial spin labeling techniques. (iii) If fresh spins travel into the imaging slice after TI, but before TR, magnetization of blood in the imaging slice recovers to M_0 by the inflow before the application of the next inversion pulse. Under a condition of $\mathrm{TI} < t_{\mathrm{transit}} < \mathrm{TR}$, where t_{transit} is the transit time of fresh blood from the edge of the inversion slab to an imaging voxel, M_z of blood will be $(1-2\,e^{-\mathrm{TI}/\mathrm{T}_{1,b}})$, which is the condition for the SI-VASO technique.

To estimate VASO and SI-VASO contrasts, computer simulations were performed using Eq. (1) at corresponding blood nulling points for various TR values, ignoring T_2^* decay. Functional signal changes that were normalized by the fully relaxed signal (i.e. $\Delta S/S_0$) and normalized by the baseline signal (i.e. $\Delta S/S$) were calculated, assuming a functional CBV increase from 5% to 5.5%. The T_1 of blood (tissue) water used for calculation was 1.35, 1.63, and 2.2 s (1.0, 1.3, and 1.9 s) at 1.5, 3, and 9.4 T, respectively (Lu et al., 2003; Lu and van Zijl, 2005; Tsekos et al., 1998). The proton densities of blood and tissue water are 0.87 and 0.89 g/ml, respectively (Lu et al., 2003). To optimize the contrast-to-noise ratio (CNR) in VASO and SI-VASO at 9.4 T, simulations were also performed using Eq. (1) as a function of TI for TR values from 2.5 to 5 s.

Animal procedure and MR methods

Five SI-VASO and spin-echo (SE)-BOLD experiments were performed on four adolescent cats (one animal was used twice) under an animal protocol approved by the Institutional Animal Care and Use Committee at the University of Pittsburgh. Details of the animal preparation procedure have been described previously (Jin et al., 2006b; Zhao et al., 2006). Briefly, the animals were first anesthetized and intubated. The cephalic vein was cannulated to deliver maintenance fluid and pancuronium bromide at ~0.2 mg/kg/hr. The end-tidal CO_2 level was kept within 3.5 ± 0.5% by slowly adjusting the respiration rate and volume, and rectal temperature was automatically controlled at 38.5 ± 0.5 °C using a water-circulating pad. During MR experiments, animals were artificially ventilated under 0.8–1.2% isoflurane in a 2:1 air: O_2 mixture. Their heads were fixed using a homemade head frame with bite and ear bars. Animals were presented binocularly with high contrast drifting square-wave gratings (2 cycles/s and 0.15 cycle/degree) during the stimulation condition. Stationary gratings of the same spatial frequency were presented during the control condition.

All MRI experiments were performed on a 9.4 T/31 cm magnet (Magnex, UK), interfaced to a Unity INOVA console (Varian, Palo Alto, CA). The actively shielded 12-cm diameter gradient insert (Magnex, UK) operates at a maximum gradient strength of 40 gauss/cm with a rise time of 130 μs. An actively detuned two-coil system was used with a homemade Helmholtz head coil (6.5 cm distance between 6.5 cm × 7 cm rectangular-shaped elements) for

inversion and a 1.6-cm diameter surface coil for both excitation and reception. From a multi-slice scout fMRI study, an axial slice showing robust activation and good-quality echo-planar image (EPI) was chosen for subsequent fMRI studies, and a T_1-weighted inversion recovery SE-EPI with a 128×128 matrix was obtained for anatomical reference.

For fMRI studies, images were acquired using the two-shot EPI technique with a center-out phase-encoding scheme and a navigator echo to achieve short TE for the SI-VASO study (Kim et al., 1996). Imaging parameters were slice thickness=2 mm, FOV=2×2 cm^2, and matrix size=64×64. SI-VASO and SE-BOLD fMRI experiments were performed in an interleaved manner. For SI-VASO, gradient-echo (GE)-EPI was used to obtain the shortest possible TE value of 3.3 ms for reducing the BOLD effects. The functional sensitivity is highly dependent on inversion slab thickness and TR/TI values; a TR per segment/TI of 2.5/1.05 s and an inversion slab of 6 cm were chosen based on pilot studies. A Gaussian-shaped adiabatic pulse with an R value of 100 was used for inversion (Garwood and DelaBarre, 2001). For SE-BOLD experiments, the double SE-EPI sequence was used with adiabatic full and half-passage pulses (TR=2.5 s per segment; TE=40 ms) (Lee et al., 1999). Temporal resolution was 5 s for both studies. For each fMRI trial, the block-design stimulation paradigm consisted of 10 control (50 s), 8 stimulation (40 s), and 20 control (100 s) images. About 25 trials were averaged for both SI-VASO and SE-BOLD fMRI to improve the SNR. In our group's previous CBV-weighted fMRI studies with an injection of 10 mg/kg MION (n=5), four-shot GE echo-planar images were obtained with TR=1 s/segment, TE=10 ms, matrix size=128×128, and stimulation duration=40 s. Details can be found in Zhao et al. (Zhao et al., 2006).

Data analysis

Data were analyzed with Matlab® programs and STIMULATE software (Strupp, 1996). To initially detect the activation area, Student's t-test maps were calculated on a pixel-by-pixel basis with a t-value threshold of 2.0 (p<0.03, uncorrected) and a minimal cluster size of 3 pixels. All quantitative analyses were performed within regions of interest (ROI) without considering whether pixels are active. The percentage signal change and CNR were analyzed as a function of cortical depth (Zhao et al., 2004). Rectangular sections within area 18 of the visual cortex were first selected. Pixels then were spatially interpolated along the direction normal to the cortical surface using the nearest-neighbor resampling method with a nominal resolution of 78 μm. Finally, signal changes were averaged across all pixels with the same cortical depth and then plotted as a function of distance from the surface of the cortex. CNR was obtained from the signal change between the 2nd–8th images of the stimulated state and the 1st–10th of the pre-stimulation control state divided by the temporal standard deviation of the control state. A full width at half maximum (FWHM) across the cortex was determined by fitting the cortical-depth fMRI response profiles to a Lorentzian function. For temporal analysis, the middle cortical ROI was hand-traced on the activation area, with ~2 pixel thickness (~4 pixels for the high resolution MION-fMRI study) to encompass approximately the middle 1/3 of gray matter, and the same ROI was used for both SI-VASO and SE-BOLD fMRI. To compare our results with previously published data, high-resolution GE CBV-weighted fMRI data with contrast agents (Zhao et al., 2006) were reanalyzed similarly to our low-resolution SI-VASO data.

Results

Computer simulation

Assuming CBV increases from 5% to 5.5% during activation, expected $\Delta S/S_0$ values (an indication of CNR) of VASO and SI-VASO signals at blood nulling points are presented in Fig. 1. Dashed lines were calculated for VASO and solid lines for SI-VASO. Clearly, $\Delta S/S_0$ of VASO decreases with a shorter TR and with a higher magnetic field strength. For TR=2.5 s, the decrease of tissue signal induced by increased CBV is only 0.015% of the fully relaxed signal (S_0) at 9.4 T when the blood signal is nulled. In contrast, the CNR of SI-VASO increases with a shorter TR, which is an order of magnitude higher for TR <3 s at 9.4 T compared to the VASO CNR.

Stimulation-induced signal changes of VASO and SI-VASO signals at 9.4 T are shown in Fig. 2 as a function of TI for several TRs. The functional contrasts change from positive to negative at TI points where signals of tissue and blood cancel each other (baseline S→0). These contrast transition points are close to the respective tissue nulling points and are shortened with decreasing TR for both VASO and SI-VASO. Although the VASO image is generally acquired at a blood nulling TI, the functional contrast as shown in Fig. 2A can be enhanced at a longer TI of ~2.1 s. This agrees with a preliminary study at 3 T in which VASO CNR at TR=2 s increased by 1.7-fold when the TI value was about two times the blood nulling point (Wu et al., 2006). In contrast, the functional contrast is only weakly dependent on the TI values for SI-VASO (Fig. 2B). Within the condition of TI <$t_{transit}$ <TR, TI should be longer than the contrast transition point to get negative fMRI contrast, and TR should be short to improve CNR. In a pilot fMRI study, the inversion slab thickness was selected as 2, 4, and 6 cm (limited by the size of the head coil). For each slab thickness, three or four TRs were used between 2 and 4.5 s, with TI values of ~200 ms larger than the respective tissue nulling points. The combination of slab thickness=6 cm, TR=2.5 s, and TI=1.05 s gave the highest CNR, and was chosen for the SI-VASO protocol in this study. At TR=2.5 s, SI-VASO has a much better contrast than VASO (see Fig. 2A vs. Fig. 2B) for most TI values. To

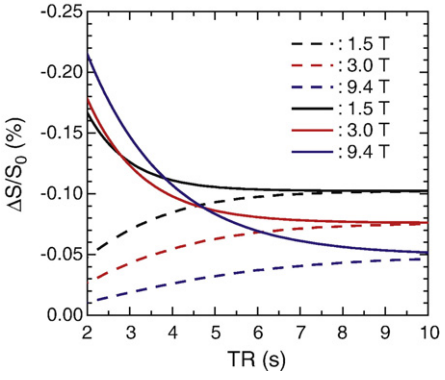

Fig. 1. Normalized fMRI contrast calculated as a function of TR at corresponding blood nulling points for VASO and SI-VASO, assuming an absolute CBV change from 5% to 5.5% during stimulation. For simulations with Eq. (1) at three different magnetic fields, T_1 values of blood and tissue were obtained from literature (see text). The T_2^* effects were ignored. The dashed and solid lines represent results for VASO and SI-VASO, respectively.

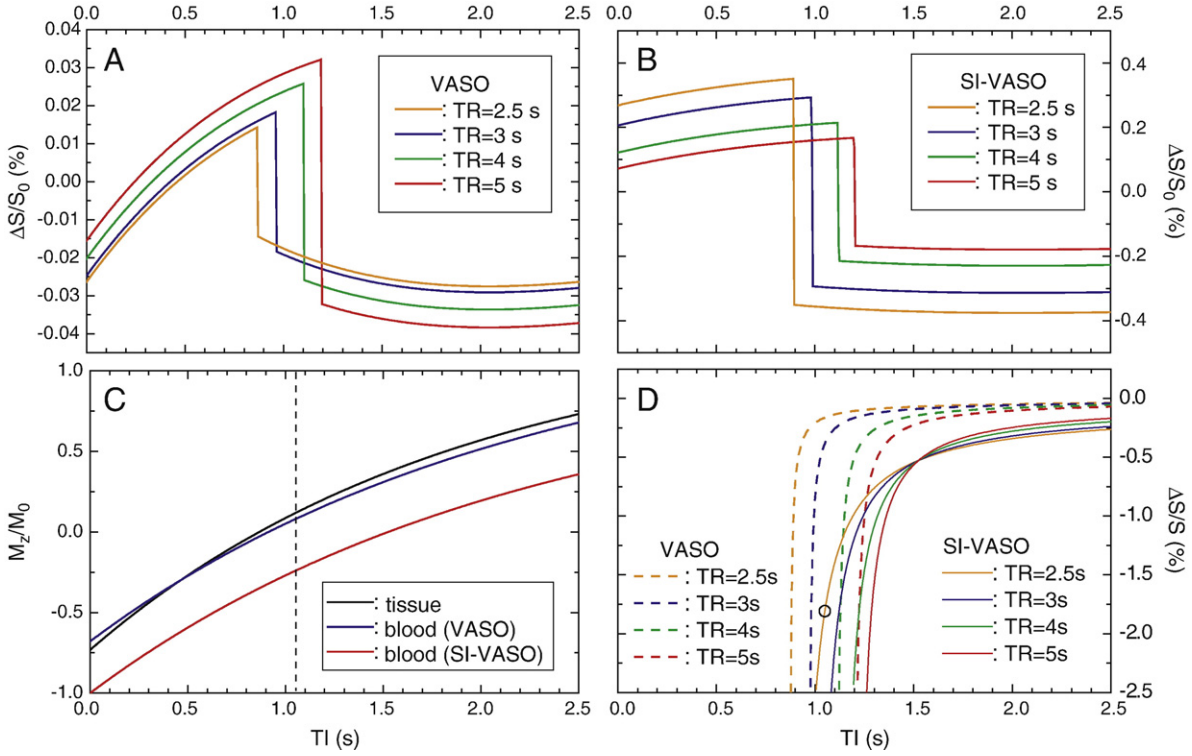

Fig. 2. Normalized fMRI contrast at 9.4 T calculated for VASO (A) and SI-VASO (B) as a function of TI for several TR values, assuming absolute CBV increases from 5% to 5.5% during stimulation. Even though VASO typically sets TI at a blood nulling point, TI was varied for simulations with Eq. (1) to determine the optimal sensitivity. Normalized longitudinal magnetizations of tissue and blood water for VASO and SI-VASO are shown in panel C as a function of TI for TR = 2.5 s. To compare with experimental results, the percentage signal change was simulated (D). In our experimental SI-VASO protocol with TR/TI = 2.5 s/1.05 s, the simulated percentage signal change is −1.8% (black circle).

compare VASO and SI-VASO signals, longitudinal magnetizations of tissue (which were the same for VASO and SI-VASO) and blood water are plotted in Fig. 2C. The steady state magnetization of blood in VASO is very close to that of tissue water, while in SI-VASO the blood magnetization is very different from tissue magnetization, enhancing the signal intensity at the blood nulling point. Fig. 2D shows the relative signal change for VASO (dashed lines) and SI-VASO (solid lines). Similar to $\Delta S/S_0$, the polarity of $\Delta S/S$ changes at TIs in which tissue and blood signals cancel (Gu et al., 2006). For simplicity, only negative signal change portions are displayed. At blood-nulling TIs, a percentage signal change is about −0.53% when absolute CBV change increases from 5% to 5.5%. For VASO, the magnitude of percentage signal change at any given TI value increases with increasing TR, but for fixed TR it decreases with increasing TI and is close to zero at TI > 1.5 s. With same TR, percentage signal change in SI-VASO is higher than that in VASO at all TI values. When absolute CBV increases from 5% to 5.5%, a percent age change in SI-VASO with TR/TI = 2.5 s/1.05 s will be −1.8% (indicated by the black circle).

Spatial specificity of VASO vs. SE-BOLD

Figs. 3A and B presents SE-BOLD and SI-VASO statistical maps overlaid on baseline EPI images obtained from one representative animal. In baseline images, the cerebrospinal fluid (CSF) signal is highest in the SE image, but nearly nulled in the SI-VASO image. In Fig. 3A, activated pixels with positive SE-BOLD signals are widespread and cover a large portion of the gray matter (outlined by the green contour). For SI-VASO, activated pixels were observed with negative changes only, predominantly at the middle of the visual cortex as indicated by the arrows. This observation agrees well with the CBV-weighted functional map using MION (Fig. 3D, with higher in-plane resolution of 156 × 156 μm^2) (Zhao et al., 2006). To directly compare two functional maps with different sensitivity, the statistical threshold of SE-BOLD fMRI was raised to match the number of activation pixels in SI-VASO (Fig. 3C). Nonetheless, SE-BOLD signals are still more spread along the cortical depth.

Cortical-depth profiles were obtained from two rectangular ROIs shown in Fig. 3E and plotted in Fig. 4A. In the baseline T_1-weighted inversion recovery image (Fig. 3E), a slightly bright band can be seen in the middle of the gray matter (red arrows), presumably indicating layer IV/Duvernoy layer 3 (Duvernoy et al., 1981; Payne and Peters, 2002). Similar MR detection of layer IV has been observed in the visual cortex of monkey and human (Goense and Logothetis, 2006; Walters et al., 2003). $\Delta S/S$ of SE-BOLD varies between a narrow range of 0.5% and 0.8% across the cortex, and FWHM of the profile is ~2.5 mm. There is a small valley at the middle cortical layer (highlighted by yellow), similar to the observation in high resolution SE-BOLD studies (Zhao et al., 2006). The negative SI-VASO signal peaks at ~0.9 mm from the cortical surface and is localized to the middle cortical layer. This agrees extremely well with the peak position of MION-fMRI (indicated by the green squares) (Zhao et al., 2006). However, the FWHM of SI-VASO fMRI is ~1.7 mm, while that of MION-fMRI is 0.81 mm. Notice that a large negative percentage change at the

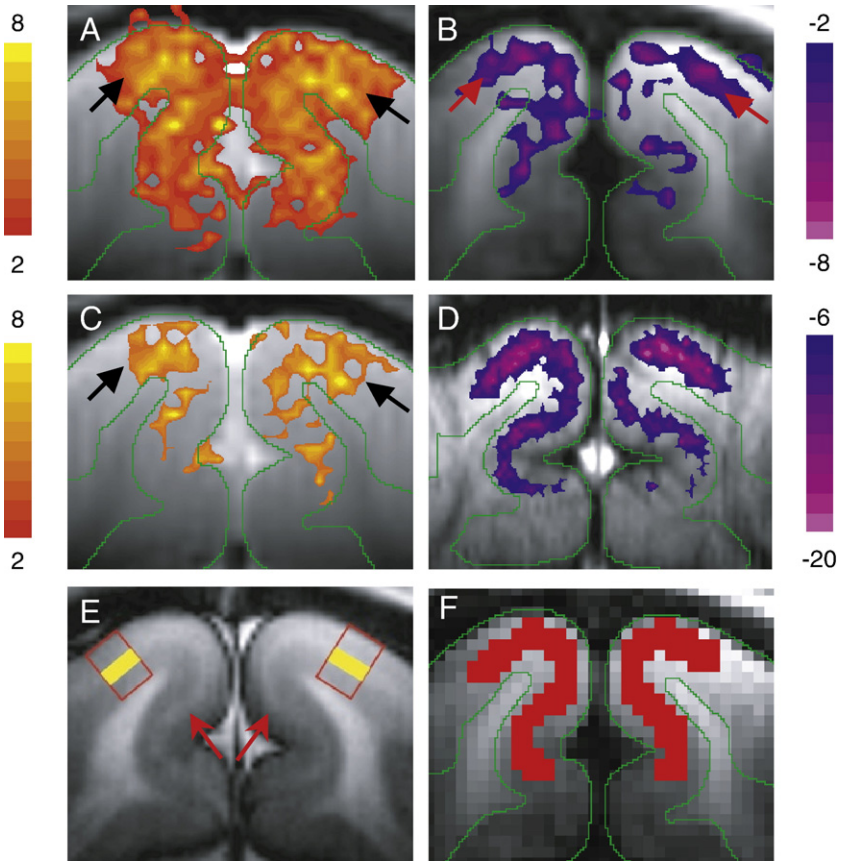

Fig. 3. Functional maps overlaid on baseline EPI images (A–D) and demarcation of ROIs (E–F). Statistical maps of SE-BOLD (A and C) and SI-VASO (B) were obtained in one representative animal, while CBV-weighted fMRI map (D) with MION was obtained from previous high-resolution data (Zhao et al., 2006). Since the sensitivity of SE-BOLD and MION-fMRI is higher than that of SI-VASO, active pixels are less for SI-VASO than for SE-BOLD and MION-fMRI when the same statistical threshold is used. Thus, to compare the spatial specificity of SI-VASO, same-sized activation pixels with the highest statistical values were chosen for SE-BOLD (C) and MION-fMRI (D). Color scales are *t*-values; *t*-value threshold used is 2.0 for (A) and (B), 3.5 for (C) and 5.5 for (D). Negative signal changes were observed in SI-VASO and MION-fMRI, while positive change was detected in SE-BOLD. The gray matter area of the visual cortex was outlined in green, and the middle of the cortex was indicated approximately by the arrows. To determine cortical depth profiles, two rectangular ROIs were selected from the T_1-weighted image (E), where white matter is brighter than gray matter, and within gray matter, layer IV/Duvernoy layer 3 has slightly higher intensity (red arrows). Yellow-highlighted region within the rectangles approximately indicates layer IV obtained from literature (Payne and Peters, 2002). The middle cortical ROI (F) was overlaid on EPI image for time course analysis. (For interpretation of the references to colour in this figure legend, the reader is referred to the web version of this article.)

cortical surface was observed in the SI-VASO profile with a large standard deviation. The cortical depth dependence of CNR (Fig. 4B) is similar to the percentage signal changes in Fig. 4A. Across the cortex, the CNR of SE-BOLD fMRI is higher than that of SI-VASO fMRI, but the CNR difference between SE-BOLD and SI-VASO fMRI is smaller at the middle cortical layer than at the upper and deeper layers. The FWHM of SI-VASO is 1.3 mm for the CNR profile, slightly narrower than the percentage signal change profile.

Temporal characteristics of SI-VASO vs. SE-BOLD

Time courses of SI-VASO and SE-BOLD fMRI were obtained at the middle cortical ROI as shown in Fig. 3F. Averaged time courses ($n=5$) are plotted in Fig. 5A. For SE-BOLD, the percentage signal change is ~0.75%, leading to a functional ΔR_2 of $-0.19\ s^{-1}$, which is in good agreement with previous results in the same animal model (Jin et al., 2006b; Zhao et al., 2004). The percentage signal change for the SI-VASO contrast is about −1.45%, which is about 80% of the simulated value in Fig. 2D where a CBV change of 0.5% is assumed. Fig. 5B shows the normalized time courses as well as MION-fMRI results (with less post-stimulus data points). Notice the time courses of the two CBV-weighted fMRI are quite similar even though they were obtained from different studies. It appears that SI-VASO responds slightly faster than SE-BOLD fMRI, but due to the limited temporal resolution, no significant difference was detected in onset time and time-to-peak. Significant post-stimulus undershoot is observed for SE-BOLD fMRI, while the SI-VASO signal returns to baseline faster without any significant undershoot, similar to the time course of MION-fMRI with similar experimental settings (Yacoub et al., 2006; Zhao et al., 2006).

Discussions

Source of SI-VASO signal

VASO contrast decreases at a higher magnetic field and a shorter TR. Thus, VASO studies reported in the literature have been performed only at 1.5 or 3 T. Our simulation results show that SI-

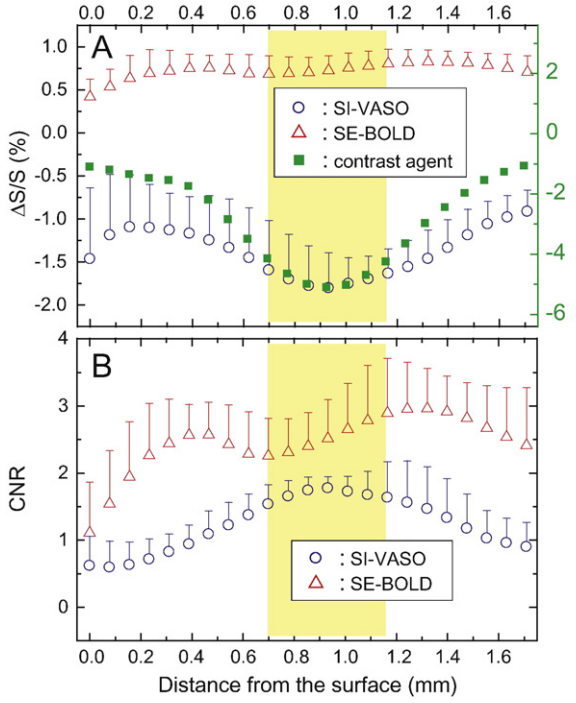

Fig. 4. Averaged cortical depth profiles ($n=5$) of SI-VASO (blue circles) and SE-BOLD responses (red triangles). Both the percentage signal change (A) and CNR (B) are shown as a function of distance from the surface of the cortex. In addition, cortical depth profile was similarly obtained from previously acquired MION-fMRI data (green squares and *Y*-axis shown in A). Yellow-highlighted region indicates the cortical layer IV (Payne and Peters, 2002); error bars (only one side is shown) represent one standard deviation. (For interpretation of the references to colour in this figure legend, the reader is referred to the web version of this article.)

VASO can be used to achieve fMRI contrast at 9.4 T. In an ideal SI-VASO case, fresh blood water spins from outside the inversion slab fill the vasculature within the imaging slice only after each image acquisition but before the next inversion pulse. Practically, the inflow of fresh blood during the time period between TI and TR may not fully fill the entire vasculature within the imaging slice, especially in downstream venous vessels. Therefore, the SI-VASO signal for a relatively short TR may be heavily weighted by the arterial CBV change. Even though the thickness of the inversion slab was varied to maximize CNR in our pilot studies, its optimization is limited due to the size of our head coil (~7 cm in slab-selection direction). To satisfy the assumption of TI < $t_{transit}$, a TI of 1.05 s was chosen instead of the blood nulling point (~1.52 s). Stimulation-induced change in inflow during the TR period will modulate tissue magnetization due to exchange between capillary and tissue water spins. In our computer simulations (Figs. 1 and 2), the exchange between blood and tissue water was ignored for the simplicity of modeling. When the exchange model is adopted as described by Lu et al. (2003), the cerebral blood flow (CBF) contribution can be estimated for our experimental conditions. Assuming that the CBV is 5% (5.5%), CBF is 100 ml/100 g/min (150 ml/100 g/min), and the water exchange fraction (E_f) is 1 (0.8) for the baseline (stimulated) states, respectively, the increase in CBF accounts for about 23% of the total SI-VASO signal. Further systematic studies are necessary to examine the source of SI-VASO signals.

In the original VASO technique, the functional signal is more weighted by arterial CBV change due to the water exchange between capillary and tissue ($E_f \neq 0$). When the exchanged water in capillaries drains into venous vasculature during the TI period, the longitudinal magnetization of the venous blood is no longer completely nulled and becomes closer to that of tissue water. Hence, the contribution of venous CBV changes to functional VASO signals is reduced even though venous CBV change is likely to be small (Kim et al., 2007). Assuming no inflow and no exchange effect, the relative CBV increase can be calculated from VASO fMRI, but the results have been found to be strongly dependent on the spatial resolution. The CBV change was reported to be ~32% at low resolution (~$3.4\times3.4\times5$ mm^3) (Gu et al., 2006), between 56% and 69% at $2\times2\times5$ mm^3 (Lu and van Zijl, 2005; Zimine et al., 2005), and up to 83% at $0.78\times0.78\times3$ mm^3 (Lu et al., 2005). These values are significantly larger than literature values obtained from other methodologies (mostly less than 30%), such as visual or somatosensory stimulation in anesthetized animals using contrast agent-based CBV methods (Mandeville et al., 2001; Zhao et al., 2006), and visual stimulation or hypercapania in humans measured by MRI or positron emission tomography (Belliveau et al., 1991; Ito et al., 2003, 2001; Rostrup et al., 2005). The high CBV change obtained from the VASO technique can be partially explained by the contribution of

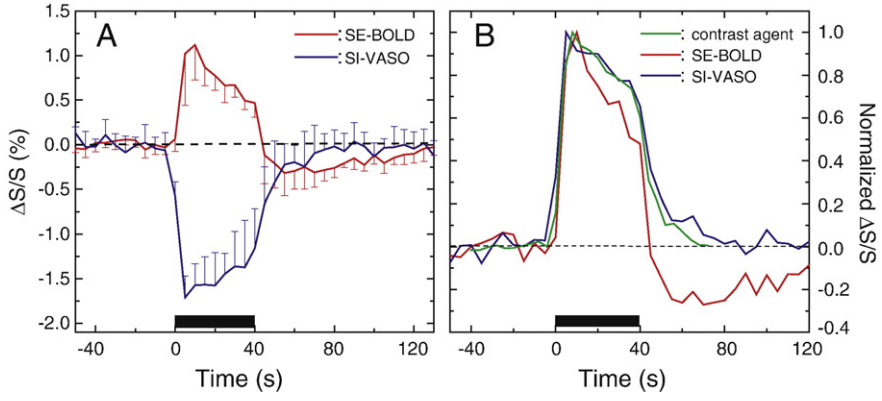

Fig. 5. Averaged raw (A) and normalized (B) time courses of SI-VASO (blue) and SE-BOLD signals (red), obtained from the middle cortical ROI shown in Fig. 3F. The normalized time course of CBV-weighted fMRI with MION was similarly obtained from a previous study in the same animal model for comparison (green curve in B). The black bar indicates the stimulation period; error bars (only one side is shown) represent one standard deviation. (For interpretation of the references to colour in this figure legend, the reader is referred to the web version of this article.)

inflowing refreshed blood if the coverage of the nonselective inversion pulse is limited (Donahue et al., 2006). An additional contamination of the VASO contrast is the extravascular BOLD signal, which reduces functional negative VASO signals due to the use of a relatively long TE (note that the intravascular BOLD contribution will not be evident with ideal blood nulling). When the BOLD contribution was reduced by a half-Fourier acquisition single-shot turbo spin echo readout (with an echo spacing of 3.5 ms and TE value of 14 ms) instead of EPI readout (TE = 11 ms), the VASO contrast was enhanced by 43% at 3 T (Poser and Norris, 2007). The extravascular BOLD contribution to VASO signal can be examined by performing experiments with multiple TE values (Lu and van Zijl, 2005) but with the same TI and TR.

We assumed minimal BOLD effects with a short TE of 3.3 ms and did not observe any positive signal changes in SI-VASO fMRI maps. The extravascular BOLD contribution is linearly dependent on TE, and thus will be minimal. However, because the intravascular BOLD contribution is closely dependent on blood T_2^* change and baseline venous blood signal intensity, it can be significant under our experimental settings because the images were not acquired at the blood nulling point and T_2^* of venous blood is very short at 9.4 T (see simulation data in (Duong et al., 2003). The intravascular BOLD contribution is highly dependent on the water exchange fraction, and can either enhance or reduce negative SI-VASO fMRI signal changes for the following two scenarios: (i) Assuming that blood and tissue are non-exchangeable compartments during the TI period (E_f=0), venous blood magnetization at TI = 1.05 s will be −0.24 M_0, while tissue magnetization will be 0.08 M_0 (dashed line in Fig. 2C). The intravascular BOLD effect will increase the magnitude of negative VASO signals. (ii) If the magnetization of venous blood water is assumed to be well mixed with the magnetization of tissue water (E_f = 1), the venous blood magnetization would be close to that of tissue (0.08 M_0). For $E_f > 0.75$, the longitudinal magnetization of venous blood would be positive, and the BOLD effect would reduce the magnitude of the negative SI-VASO signal change. Under our experimental conditions, the intravascular BOLD effect is expected to be small for E_f between 0.6 and 0.9 because the longitudinal magnetization of venous blood would be less than 5% of M_0.

Spatial specificity of SI-VASO signals

The SI-VASO results show some similarities but also differences with CBV-weighted fMRI using MION. Despite different CNRs, the negative signal change of both methods peaks at the middle cortical layer. When relative CBV change is estimated from SI-VASO fMRI data (−1.45%) and Eq. (1) with our experimental parameters, it is ~8% (assuming baseline CBV of 5%), which agrees with the CBV change obtained using MION-fMRI in the same animal model, ~8% when averaged across the middle cortical layer (Zhao et al., 2006). However, the FWHM of SI-VASO is about twice that of MION-fMRI. This difference may be due to slightly different signal sources and different BOLD contributions. SI-VASO is more weighted by changes in arterial blood vessels when TR is short, while CBV-weighted fMRI using MION is sensitive to changes in all sizes of arterial and venous vessels. As mentioned before, inflow and intravascular BOLD effects will contribute to SI-VASO fMRI, but not in MION-fMRI studies because of the short T_2^* after MION injection. In contrast, the extravascular BOLD effect will be minimal in SI-VASO with TE = 3.3 ms, but is more significant in the MION-fMRI study with TE = 10 ms. Inflow and intravascular BOLD contributions to SI-VASO may broaden its FWHM, whereas the extravascular BOLD contribution to MION-fMRI was found to artificially narrow the true FWHM of CBV response (0.92 mm with BOLD correction vs. 0.81 mm without BOLD correction; (Zhao et al., 2006)).

It is worthwhile to note that the CBV-weighted fMRI signal also can be obtained from diffusion-weighted fMRI studies with $b < 200$–300 s/mm^2 (Jin et al., 2006c). Based on computer simulations and experimental data at 9.4 T, functional apparent diffusion coefficient (ADC) changes with small b-values are heavily weighted by arterial CBV changes when the intravascular BOLD contribution is minimized at a sufficiently long TE. We have found that the increase of ADC during stimulation peaks at the middle cortical layer with a FWHM of ~1 mm (Jin et al., 2006c). Because both SI-VASO and ADC fMRI exhibit arterial CBV-weighting, it will be interesting to compare these two methods in the same subjects.

Compared to SE-BOLD with a lamina FWHM of ~2.5 mm, the SI-VASO signal is better localized to the middle cortical layer. Our SE-BOLD vs. SI-VASO observation is consistent with previous SE-BOLD vs. MION-fMRI data (Zhao et al., 2006). The CBV-weighted fMRI response peaks at ~0.9 mm from the cortical surface where the baseline R_2 change is also highest after MION injection, whereas the SE-BOLD response is relatively broad with a small valley at the middle cortical layer (Zhao et al., 2006). At high magnetic fields, SE-BOLD is sensitive to signal changes in small-sized vessels and surrounding tissue. Based on previous SE-BOLD fMRI experiments with TE = 40 ms at 9.4 T (Lee et al., 1999), the extravascular BOLD contribution around small-sized vessels is dominant. But at lower magnetic fields, the intravascular BOLD signal from all sizes of deoxyhemoglobin-containing vessels contributes, reducing the spatial specificity of SE-BOLD. In contrast, because the SI-VASO fMRI signal is likely to reflect changes in physiological parameters and is not a susceptibility-based contrast, its spatial specificity is expected to be similar across magnetic fields. Moreover, BOLD contributions to VASO-based fMRI will be less at lower magnetic fields, and can possibly be further reduced with different imaging acquisition schemes. Thus, SI-VASO fMRI will potentially be more advantageous over SE-BOLD fMRI at lower fields (≤3 T).

The lamina profile of our SE-BOLD agrees well with previous high-resolution studies from our group (Zhao et al., 2006). Based on similar cat visual stimulation studies, Harel et al. found the highest CBV change at a small valley in the SE-BOLD cortical profile (which is consistent with our observation), but assigned the region with the highest SE-BOLD change to layer IV (Harel et al., 2006). Goense et al. also reported that SE-BOLD peaked at the middle of the V1 cortex of monkey at 4.7 T (Goense and Logothetis, 2006), where the change in R_2 was found to be the highest after MION injection (Goense et al., 2007). A significant contribution of functional T_2^* change to SE-BOLD fMRI during a long readout time may shift the peak of the lamina response because the T_2^* contribution of pial veins monotonically decreases along cortical depth. Based on our previous multiple TE SE-BOLD studies of cat visual cortex (Jin et al., 2006b), the contribution of T_2^* change is not significant at 9.4 T for single-shot SE-BOLD fMRI with a readout time of 32 ms. Because the acquisition window (~12 ms) for two-shot EPI is much shorter than the tissue T_2^* value (~30 ms at 9.4 T), T_2^* contamination should be very small in our SE-BOLD data, and is unlikely a source of discrepancy between our study and others. The apparent discrepancy may be due to slight differences in the choice of ROIs for profile

analysis and/or in the choice of layer boundaries. Further investigations will be needed to address these issues.

Temporal characteristics of SI-VASO

With MION-fMRI, it was reported in rodent and monkey that the CBV response is slower than BOLD for onset time, time-to-peak, and time-to-recovery after the offset of stimulation (Leite et al., 2002; Mandeville et al., 1998). In isoflurane-anesthetized cat visual stimulation studies, the CBV and BOLD responses are highly dependent on the choice of ROI. The CBV response is slightly faster than BOLD at the surface vessel area but slower at the middle of the cortex (Jin et al., 2006a; Yacoub et al., 2006). For human visual stimulation, the CBV response measured with the VASO technique is faster than the BOLD signal change (Lu et al., 2004a) in onset (rising) time. Even though the low temporal resolution and the low CNR of SI-VASO prevent detailed analysis of temporal behavior, the SI-VASO signal peaks slightly faster than SE-BOLD. It also appears that the SI-VASO response peaks slightly faster than MION-fMRI, which is possibly due to slightly different signal sources (arterial CBV vs. total CBV). Nevertheless, the overall similarity in the time courses of SI-VASO and MION-fMRI indicates that SI-VASO indeed mostly reflects functional CBV change. The discrepancy reported in the literature regarding the temporal behavior of VASO and MION-fMRI (Leite et al., 2002; Lu et al., 2004a; Mandeville et al., 1998) may be attributed to slight differences in their signal sources, but factors such as spatial location, species, anesthesia, stimulation type, and duration also may be contributing factors. In our current data, the time-to-peak of CBV response is shorter than that observed by Mandeville and colleagues (Leite et al., 2002; Mandeville et al., 1998), which is likely due to different stimulation paradigms. More direct comparison of SI-VASO and MION-fMRI would require that the two methods be performed on the same subjects during various stimulations with improved SI-VASO temporal resolution.

Conclusions

We have demonstrated that SI-VASO can be used to obtain functional contrast at 9.4 T. This SI-VASO method enhances CNR compared to the original VASO technique, especially at high magnetic fields and short TRs. The exact source of the SI-VASO signal is highly dependent on slab thickness and TR and TI values. The SI-VASO signal may be more weighted by the CBV change from the arterial side of the vasculature and have significant contributions from CBF and blood oxygenation changes. Compared to SE-BOLD, SI-VASO shows better spatial specificity to the middle cortical layer, albeit slightly lower CNR. Therefore, it may be a useful tool for high-resolution functional brain mapping in humans.

Acknowledgments

This work is supported by NIH grants EB003324, EB003375, and NS44589. The 9.4 T MRI system was funded in part by NIH Grant RR17239. We thank Fuqiang Zhao for providing high-resolution MION-fMRI data, Jicheng Wang for building an actively-detunable Helmholtz head coil, Michelle Tasker and Ping Wang for animal preparation, Kristy Hendrich for maintaining the 9.4 T system, and Joseph Mandeville at Massachusetts General Hospital for helpful discussions of CBV dynamics.

References

Belliveau, J.W., Kennedy, D.N., McKinstry, R.C., Buchbinder, B.R., Weisskoff, R.M., Cohen, M.S., Vevea, J.M., Brady, T.J., Rosen, B.R., 1991. Functional mapping of the human visual cortex by magnetic resonance imaging. Science 254, 716–719.

Donahue, M.J., Lu, H.Z., Jones, C.K., Edden, R.A.E., Pekar, J.J., van Zijl, P.C.M., 2006. Theoretical and experimental investigation of the VASO contrast mechanism. Magn. Reson. Med. 56, 1261–1273.

Duong, T.Q., Yacoub, E., Adriany, G., Hu, X., Ugurbil, K., Kim, S.-G., 2003. Microvascular BOLD contribution at 4 and 7 T in the human brain: gradient-echo and spin-echo fMRI with suppression of blood effects. Magn. Reson. Med. 49, 1019–1027.

Duvernoy, H., Delon, S., Vannson, J., 1981. Cortical blood vessels of the human brain. Brain Res. Brain 7, 519–579.

Fukuda, M., Moon, C.H., Wang, P., Kim, S.G., 2006. Mapping iso-orientation columns by contrast agent-enhanced functional magnetic resonance imaging: reproducibility, specificity, and evaluation by optical imaging of intrinsic signal. J. Neurosci. 26, 11821–11832.

Garwood, M., DelaBarre, L., 2001. The return of the frequency sweep: designing adiabatic pulses for contemporary NMR. J. Magn. Reson. 153, 155–177.

Goense, J.B.M., Logothetis, N.K., 2006. Laminar specificity in monkey V1 using high-resolution SE-fMRI. Magn. Reson. Imaging 24, 381–392.

Goense, J.B.M., Zappe, A.-C., Logothetis, N.K., 2007. High-resolution fMRI of macaque V1. Magn. Reson. Imaging 25, 740–747.

Gu, H., Lu, H.Z., Ye, F.Q., Stein, E.A., Yang, Y.H., 2006. Noninvasive quantification of cerebral blood volume in humans during functional activation. NeuroImage 30, 377–387.

Harel, N., Lin, J., Moeller, S., Ugurbil, K., Yacoub, E., 2006. Combined imaging-histological study of cortical laminar specificity of fMRI signals. NeuroImage 29, 879–887.

Ito, H., Takahashi, K., Hatazawa, J., Kim, S.-G., Kanno, I., 2001. Changes in human regional cerebral blood flow and cerebral blood volume during visual stimulation measured by positron emission tomography. J. Cereb. Blood Flow Metab. 21, 608–612.

Ito, H., Kanno, I., Ibaraki, M., Hatazawa, J., Miura, S., 2003. Changes in human cerebral blood flow and cerebral blood volume during hypercapania and hypocapania measured by Positron Emission Tomography. J. Cereb. Blood Flow Metab. 23, 665–670.

Jin, T., Kim, S.G., 2006. Spatial dependence of CBV-fMRI: a comparison between VASO and contrast agent based methods. 28th IEEE EMBS Annual International Conference, New York, NY, pp. 25–28.

Jin, T., Wang, J., Zhao, F., Wang, P., Tasker, M., Kim, S.G., 2006a. Spatiotemporal characteristics of BOLD, CBV and CBF responses in the cat visual cortex. Proc 14th Annual Meeting, ISMRM, Seattle.

Jin, T., Wang, P., Tasker, M., Zhao, F.Q., Kim, S.G., 2006b. Source of nonlinearity in echo-time-dependent BOLD fMRI. Magn. Reson. Med. 55, 1281–1290.

Jin, T., Zhao, F.Q., Kim, S.G., 2006c. Sources of functional apparent diffusion coefficient changes investigated by diffusion-weighted spin-echo fMRI. Magn. Reson. Med. 56, 1283–1292.

Kennan, R.P., Scanley, B.E., Innis, R.B., Gore, J.C., 1998. Physiological basis for BOLD MR signal changes due to neuronal stimulation: Separation of blood volume and magnetic susceptibility effects. Magn. Reson. Med. 40, 840–846.

Kim, S.-G., Ugurbil, K., 2003. High-resolution functional magnetic resonance imaging of the animal brain. Methods 30, 28–41.

Kim, S.-G., Hu, X., Adriany, G., Ugurbil, K., 1996. Fast interleaved echo-planar imaging with navigator: high resolution anatomic and functional images at 4 Tesla. Magn. Reson. Med. 35, 895–902.

Kim, T., Hendrich, K., Masamoto, K., Kim, S.G., 2007. Arterial versus total blood volume changes during neural activity-induced cerebral blood flow change: implication for BOLD fMRI. J. Cereb. Blood Flow Metab. 27, 1235–1247.

Lee, S.-P., Silva, A.C., Ugurbil, K., Kim, S.-G., 1999. Diffusion-weighted spin-echo fMRI at 9.4 T: microvascular/tissue contribution to BOLD signal change. Magn. Reson. Med. 42, 919–928.

Leite, F.P., Tsao, D., Vanduffel, W., Fize, D., Sasaki, Y., Wald, L.L., Dale, A.M., Kwong, K.K., Orban, G.A., Rosen, B.R., Tootell, R.B.H., Mandeville, J.B., 2002. Repeated fMRI using iron oxide contrast agent in awake, behaving macaques at 3 Tesla. NeuroImage 16, 283–294.

Lu, H.Z., van Zijl, P.C.M., 2005. Experimental measurement of extravascular parenchymal BOLD effects and tissue oxygen extraction fractions using multi-echo VASO fMRI at 1.5 and 3.0 T. Magn. Reson. Med. 53, 808–816.

Lu, H., Golay, X., Pekar, J., Van Zijl, P., 2003. Functional magnetic resonance imaging based on changes in vascular space occupancy. Magn. Reson. Med. 50, 263–274.

Lu, H., Golay, X., Pekar, J., van Zijl, P.C., 2004a. Sustained poststimulus elevation in cerebral oxygen utilization after vascular recovery. J. Cereb. Blood Flow Metab. 24, 764–770.

Lu, H.B., Patel, S., Luo, F., Li, S.J., Hillard, C.J., Ward, B.D., Hyde, J.S., 2004b. Spatial correlations of laminar BOLD and CBV responses to rat whisker stimulation with neuronal activity localized by Fos expression. Magn. Reson. Med. 52, 1060–1068.

Lu, H., Donahue, M.J., Jones, C.K., Van Zijl, P.C.M., 2005. Spatial characteristics of VASO fMRI at ultra-high resolution. Proceedings of the 13th Annual Meeting of ISMRM, Miami, FL, p. 27.

Mandeville, J.B., Marota, J.J.A., Kosofsky, B.E., Keltner, J.R., Weissleder, R., Rosen, B.R., 1998. Dynamic functional imaging of relative cerebral blood volume during rat forepaw stimulation. Magn. Reson. Med. 39, 615–624.

Mandeville, J.B., Marota, J.J.A., Ayata, C., Moskowitz, M.A., Weisskoff, R.M., Rosen, B.R., 1999. MRI measurement of the temporal evolution of relative CMRO2 during rat forpaw stimulation. Magn. Reson. Med. 42, 944–951.

Mandeville, J.B., Jenkins, B.G., Kosofsky, B.E., Moskowitz, M.A., Rosen, B.R., Marota, J.J.A., 2001. Regional sensitivity and coupling of BOLD and CBV changes during stimulation of rat brain. Magn. Reson. Med. 45, 443–447.

Payne, B.R., Peters, A., 2002. The concept of cat primary visual cortex. In: Payne, B.R., Peters, A. (Eds.), The Cat Primary Visual Cortex. Academic Press, pp. 1–129.

Poser, B.A., Norris, D.G., 2007. Measurement of activation-related changes in cerebral blood volume: VASO with single-shot HASTE acquisition. Magn. Reson. Mater. Phys. 20, 63–67.

Rostrup, E., Knudsen, G.M., Law, I., Holm, S., Larsson, H.B.W., Paulson, O.B., 2005. The relationship between cerebral blood flow and volume in humans. NeuroImage 24, 1–11.

Strupp, J.P., 1996. Stimulate: a GUI based fMRI analysis software package. NeuroImage 3, S607.

Tsekos, N.V., Zhang, F., Merkle, H., Nagayama, M., Iadecola, C., Kim, S.-G., 1998. Quantitative measurements of cerebral blood flow in rats using the FAIR technique: correlation with previous iodoantipyrine autoradiographic studies. Magn. Reson. Med. 39, 564–573.

Vanduffel, W., Fize, D., Mandeville, J.B., Nelissen, K., van Hecke, P., Rosen, B.R., Tootell, R.B.H., Orban, G.A., 2001. Visual motion processing investigated using contrast agent-enhanced fMRI in awake behaving monkeys. Neuron 32, 565–577.

Walters, N.B., Egan, G.F., Kril, J.J., Kean, M., Waley, P., Jenkinson, M., Watson, J.D.G., 2003. In vivo identification of human cortical areas using high-resolution MRI: an approach to cerebral structure–function correlation. Proc. Natl. Acad. Sci. U. S. A. 100, 2981–2986.

Wu, W.-C., Wegener, S., Buxton, R.B., Wong, E.C., 2006. Vascular space occupancy weighted imaging with control of inflow effect and higher signal-to-noise ratio. ISMRM, Seattle, WA, p. 2768.

Yacoub, E., Ugurbil, K., Harel, N., 2006. The spatial dependence of the poststimulus undershoot as revealed by high-resolution BOLD- and CBV-weighted fMRI. J. Cereb. Blood Flow Metab. 26, 634–644.

Yang, Y.H., Gu, H., Stein, E.A., 2004. Simultaneous MRI acquisition of blood volume, blood flow, and blood oxygenation information during brain activation. Magn. Reson. Med. 52, 1407–1417.

Zhao, F., Wang, P., Kim, S.-G., 2004. Cortical depth-dependent gradient-echo and spin-echo BOLD fMRI at 9.4T. Magn. Reson. Med. 51, 518–524.

Zhao, F., Wang, P., Hendrich, K., Kim, S.-G., 2005. Spatial specificity of cerebral blood volume-weighted fMRI responses at columnar resolution. NeuroImage 27, 416–424.

Zhao, F., Wang, P., Hendrich, K., Ugurbil, K., Kim, S.-G., 2006. Cortical layer-dependent BOLD and CBV responses measured by spin-echo and gradient-echo fMRI: Insights into hemodynamic regulation. NeuroImage 30, 1149–1160.

Zimine, I., Petersen, E.T., Ho, Y.L., Golay, X., 2005. Partial volume effects in VASO-fMRI. Proceedings of 13th Annual Meeting of ISMRM, Miami, FL, p. 493.